

# Radial Tchebichef Invariants for Pattern Recognition

Ramakrishnan Mukundan, *Senior Member, IEEE*

**Abstract**—This paper presents the mathematical framework of radial Tchebichef moment invariants, and investigates their feature representation capabilities for pattern recognition applications. The radial Tchebichef moments are constructed using the discrete orthogonal Tchebichef polynomials as the kernel, and they have a radial-polar form similar to that of Zernike moments. The discrete form of the moment transforms make them particularly suitable for image processing tasks. Experimental results showing the primary attributes such as invariance and orthogonality of the proposed moment functions are also given.

**Index Terms**—Discrete transforms, feature extraction, image reconstruction, orthogonal functions, pattern recognition.

## I. INTRODUCTION

PATTERN recognition and other similar applications require robust feature descriptors that are invariant to rotational transformations. Zernike and Pseudo-Zernike moments have been found to have the desirable qualities of orthogonality and robustness, which could be exploited in a variety of tasks involving identification or recognition of objects [1],[2]. However, moments constructed using continuous orthogonal polynomials such as Zernike functions require a coordinate transformation to the domain of the functions, which is usually the interior of a unit circle [3],[4]. Correspondingly, a discrete approximation of the moment integrals could also introduce numerical errors in the computation of feature descriptors.

The primary motivation for developing discrete orthogonal invariants arises from the need to eliminate image coordinate transformations and the discretization step in the moment calculation. Radial Tchebichef invariants retain the basic form of Zernike moments (so that the rotational invariants can be derived easily), but use one-dimensional Tchebichef polynomials in the kernel [3], leading to a moment definition that operates directly in the image space. In other words, the most powerful characteristics of Tchebichef moments (discrete, orthogonal), and Zernike moments (rotational invariance) have been combined to create the proposed class of radial Tchebichef invariants.

This paper presents the essential framework required for the computation of radial Tchebichef moments, and investigates the properties such as orthogonality, rotational invariance, and robustness with respect to input noise. The paper is organized as follows: The next section gives the

definition of Tchebichef polynomials and moments. Radial Tchebichef moments are introduced in Section III, along with Zernike moments to make the similarities in the structure of the two types of moments evident. Section IV gives an outline of rotational invariants using radial Tchebichef moments. Key implementation aspects related to the computation of radial invariants are discussed in Section V. Experimental results demonstrating the invariance characteristics of these functions, and the reconstruction capability of the corresponding moments are given in Section VI. Concluding remarks are given in Section VII.

## II. TCHEBICHEF MOMENTS

The Tchebichef moments of order  $p+q$  of an image  $f(x, y)$  of size  $N$  are defined using the scaled orthogonal Tchebichef polynomials  $t_{p,N}()$ , as follows[5].

$$T_{pq} = \frac{1}{\rho(p, N)\rho(q, N)} \sum_{x=0}^{N-1} \sum_{y=0}^{N-1} t_{p,N}(x) t_{q,N}(y) f(x, y) \quad (1)$$

$p, q = 0, 1, \dots, N-1,$

where the polynomial functions are given by [6],

$$t_{p,N}(x) = \frac{p!}{N^p} \sum_{k=0}^p (-1)^{p-k} \binom{N-1-k}{p-k} \binom{p+k}{p} \binom{x}{k} \quad (2)$$

The scale factor  $N^p$  is introduced in the above equation to ensure numerical stability of higher order functions. The polynomials  $t_{p,N}(x)$ , satisfy the recurrence formula [7],[8]:

$$\begin{aligned} (p+1)t_{p+1,N}(x) - (2p+1)(2x-N+1)t_{p,N}(x) \\ + p(1-p^2/N^2)t_{p-1,N}(x) = 0 \end{aligned} \quad (3)$$

$p = 1, 2, \dots, N-2; \quad x = 0, 1, \dots, N-1.$

with initial conditions,

$$\begin{aligned} t_0(x) &= 1, \\ t_1(x) &= (2x-N+1)/N, \end{aligned} \quad (4)$$

The squared-norm  $\rho(p, N)$  is equivalent to

$$\sum_{x=0}^{N-1} \{t_{p,N}(x)\}^2 = \frac{N \left(1 - \frac{1}{N^2}\right) \left(1 - \frac{2^2}{N^2}\right) \dots \left(1 - \frac{p^2}{N^2}\right)}{2p+1}, \quad (5)$$

$p = 0, 1, \dots, N-1.$

The squared norm satisfies the following recurrence relation:

$$\rho(p, N) = \frac{(N^2 - p^2)(2p-1)}{N^2(2p+1)} \rho(p-1, N). \quad (6)$$

The most important property of the set  $\{t_{m,N}(x)\}$  that is utilized in a moment definition, is its orthogonality in the discrete domain[5],[9]:

$$\sum_{x=0}^{N-1} t_{p,N}(x) t_{q,N}(x) = \rho(p, N) \delta_{pq}, \quad (7)$$

which leads to an exact image reconstruction formula (inverse moment transform),

$$f(x, y) = \sum_{p=0}^{N-1} \sum_{q=0}^{N-1} T_{pq} t_{p,N}(x) t_{q,N}(y). \quad (8)$$

### III. RADIAL MOMENTS

Radial moments generally use a radial-polar coordinate system  $(r, \theta)$  and combine a one-dimensional orthogonal function in  $r$  with a circular function in  $\theta$  to form moments of an image  $f(r, \theta)$ . In this section, we first review the definition of the popular Zernike moments and then introduce radial Tchebichef moments. The primary advantage of radial moments is that rotational invariants can be easily constructed by eliminating the corresponding phase component from a moment expression.

#### A. Zernike Moments

The Zernike moments have complex kernel functions based on Zernike polynomials, and are defined as [1]

$$Z_{nl} = \frac{(n+1)}{\pi} \int_0^{2\pi} \int_0^1 R_{nl}(r) e^{-jl\theta} f(r, \theta) r dr d\theta, \quad (9)$$

where  $r \leq 1$ ,  $j = (-1)^{1/2}$ , and the function  $R_{nl}(r)$  denotes a radial Zernike polynomial of order  $n$  and repetition  $l$ . In the above equation  $n$  is a non-negative integer, and  $l$  is an integer such that  $n-|l|$  is even, and  $|l| \leq n$ . The radial Zernike polynomials are real-valued functions defined as

$$R_{nl}(r) = \sum_{s=0}^{(n-|l|)/2} (-1)^s \frac{(n-s)!}{s! \left(\frac{n-2s+|l|}{2}\right)! \left(\frac{n-2s-|l|}{2}\right)!} r^{n-2s} \quad (10)$$

The above functions are continuous and orthogonal inside the unit circle  $|r| < 1$ . This requires a coordinate transformation from the image space to the region  $[-1, 1]$ , as well as a discrete approximation of the integrals in (9).

#### B. Radial Tchebichef Moments

We can define a set of discrete orthogonal moments in a similar fashion, by combining the one-dimensional Tchebichef polynomials in (2) with a circular function. Since we use the discrete domain of the image space for

these functions (Fig. 1), we allow the parameter  $r$  to vary from 0 to  $N/2$ , and the angle  $\theta$  to vary from 0 to  $2\pi$  in  $n$  discrete steps, such that

$$\theta_k = \frac{2\pi k}{n}, \quad k = 0, 1, 2, \dots, n-1. \quad (11)$$

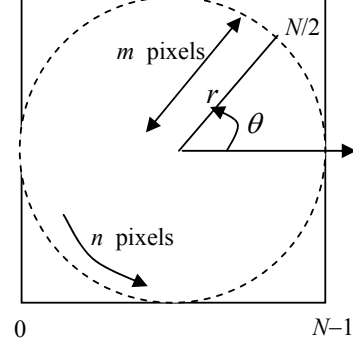


Fig. 1. Domain of definition of radial Tchebichef moment functions.

The radial Tchebichef moments of order  $p$  and repetition  $q$  are defined using the equation

$$S_{pq} = \frac{1}{n \rho(p, m)} \sum_{r=0}^{m-1} \sum_{k=0}^{n-1} t_{p,m}(r) e^{-j \frac{2\pi q k}{n}} f(r, \theta_k) \quad (12)$$

where  $m = N/2$ ,  $\theta_k$  is given by (11), and  $n$  denotes the maximum number of pixels along the circumference of the circle in Fig.1. The inverse moment transform is given by the following equation:

$$f(r, \theta) \approx \sum_{p=0}^{pmax} \sum_{q=1}^{qmax} S_{pq} t_{p,m}(r) e^{jq\theta} \quad (13)$$

where  $pmax$ ,  $qmax$  denote the maximum order and repetition of moments used.

The real-valued components of radial Tchebichef moments can be obtained from (12):

$$S_{pq}^{(c)} = \frac{1}{n \rho(p, m)} \sum_{r=0}^{m-1} \sum_{k=0}^{n-1} t_{p,m}(r) \cos\left(\frac{2\pi q k}{n}\right) f(r, \theta_k)$$

$$S_{pq}^{(s)} = \frac{1}{n \rho(p, m)} \sum_{r=0}^{m-1} \sum_{k=0}^{n-1} t_{p,m}(r) \sin\left(\frac{2\pi q k}{n}\right) f(r, \theta_k) \quad (14)$$

so that

$$S_{pq} = S_{pq}^{(c)} - j S_{pq}^{(s)} \quad (15)$$

With the above definitions, the inverse moment transform (13) can be conveniently expressed in terms of real-valued functions:

$$f(r, \theta) = \sum_{p=0}^{pmax} t_p(r) \left\{ S_{p0}^{(c)} + 2 \sum_{q=1}^{qmax} S_{pq}^{(c)} \cos(q\theta) + S_{pq}^{(s)} \sin(q\theta) \right\} \quad (16)$$

#### IV. ROTATIONAL INVARIANTS

Consider an image rotation by an angle  $\alpha$  about the centre of the image. Assuming that the image intensity values are preserved throughout the rotation, the Zernike moments  $Z'_{nl}$  of the transformed image are related to the moments  $Z_{nl}$  of the original image by the equation,

$$Z'_{nl} = e^{-jl\alpha} Z_{nl}, \quad n \geq 0. \quad (17)$$

Any moment expression that is independent of the parameter  $\alpha$  is obviously a rotation invariant. The primary rotation invariants of Zernike moments are

$$\varphi_n = Z_{n0}; \quad \varphi_{nl} = |Z_{nl}|^2, \quad (18)$$

where  $n \geq 0$ , and  $n - |l|$  is even. Similarly, we can write invariants of radial Tchebichef moments in the form

$$\begin{aligned} \eta_p &= S_{p0} = S_{p0}^{(c)} \\ &= \frac{1}{n \rho(p, m)} \sum_{r=0}^{m-1} \sum_{k=0}^{n-1} t_{p,m}(r) f(r, \theta_k) \end{aligned} \quad (19)$$

$$\eta_{pq} = |S_{pq}|^2 = \left(S_{pq}^{(c)}\right)^2 + \left(S_{pq}^{(s)}\right)^2, \quad q > 0. \quad (20)$$

#### V. IMPLEMENTATION ASPECTS

As the parameters  $r$  and  $t$  are varied in (14), we require the Cartesian coordinates of the image pixel at the corresponding location, in order to obtain the intensity value. The pixel position can be obtained using the equations

$$\begin{aligned} x &= \frac{rN}{2(m-1)} \cos\left(\frac{2\pi k}{n}\right) + \frac{N}{2} \\ y &= \frac{rN}{2(m-1)} \sin\left(\frac{2\pi k}{n}\right) + \frac{N}{2} \\ r &= 0, 1, 2, \dots, m-1; \quad k = 0, 1, 2, \dots, n-1. \end{aligned} \quad (21)$$

Like many image transforms, the radial Tchebichef moment equations in (14) are also separable, and this property can be used to considerably reduce the computation time. Thus the moments can be computed in a two-step process as shown below.

Step 1: Compute one dimensional Tchebichef moments along each radius vector, and store them in an array.

$$Q_p(k) = \frac{1}{\rho(p, m)} \sum_{r=0}^{m-1} t_{p,m}(r) f(r, \theta_k) \quad (22)$$

Step 2: Compute the real-valued circular moments of the above function:

$$S_{pq}^{(c)} = \frac{1}{n} \sum_{k=0}^{n-1} \cos\left(\frac{2\pi qk}{n}\right) Q_p(k) \quad (23)$$

$$S_{pq}^{(s)} = \frac{1}{n} \sum_{k=0}^{n-1} \sin\left(\frac{2\pi qk}{n}\right) Q_p(k) \quad (24)$$

Using the above scheme, the total number of iterations reduces from  $(pmax)(qmax)mn$  to  $(pmax)(qmax+m)n$ . For an image of size  $N \times N$ , the value of  $m$  is  $N/2$ , and  $n$  is approximately  $4N$ . Both  $m$  and  $n$  may be set to a higher value to improve the quality of reconstruction. The values of  $pmax$ ,  $qmax$  depend on the order of invariants required (usually less than 6), or the order of moments used for reconstruction (usually  $N/2$ ). The pseudo-code for the computation of moment invariants is given in Fig. 2 below.

```

1. Input:
   Image  $f(x, y)$ ,  $0 \leq x, y \leq N-1$ .
    $m = N/2$ ,  $n = 6N$ .
2. Compute Tchebichef polynomials:
   for ( $r=0$ ;  $r < m$ ;  $r++$ ) {
       for ( $p=2$ ;  $p < pmax$ ;  $p++$ ) {
           Compute  $t_{p,m}(r)$  using (3)
       }
   }
3. Compute norm:
   for ( $p=1$ ;  $p < pmax$ ;  $p++$ ) {
       Compute  $\rho(p, m)$  using (6)
   }
4. Compute moments - Step 1 (22):
   for ( $p=0$ ;  $p < pmax$ ;  $p++$ ) {
       for ( $k=0$ ;  $k < n$ ;  $k++$ ) {
            $\theta = 2\pi k/n$ ;
           for ( $r=0$ ;  $r < m$ ;  $r++$ ) {
               Compute  $x, y$  using (21).
               Set  $f(r, \theta) = f(x, y)$ 
               Compute  $Q_p(k)$  using (22)
           }
       }
   }
5. Compute moments - Step 2 (23)
   for ( $p=0$ ;  $p < pmax$ ;  $p++$ ) {
       for ( $q=0$ ;  $q < qmax$ ;  $q++$ ) {
           for ( $k=0$ ;  $k < n$ ;  $k++$ ) {
               Compute  $S_{pq}^{(c)}$  using (23)
               Compute  $S_{pq}^{(s)}$  using (24)
           }
       }
   }
6. Compute invariants:
   Use (19), (20) to compute invariants for any specific
   value of  $p$  and  $q$ .

```

Fig. 2. Pseudo-code for computing radial Tchebichef invariants.

#### VI. EXPERIMENTAL RESULTS

The study the invariant characteristics of radial Tchebichef moments have yielded promising results. Fig. 3 shows a sample set of binary images and their clockwise angles of rotation  $\alpha$ , used in the analysis. Each image has a size of  $120 \times 120$  pixels.

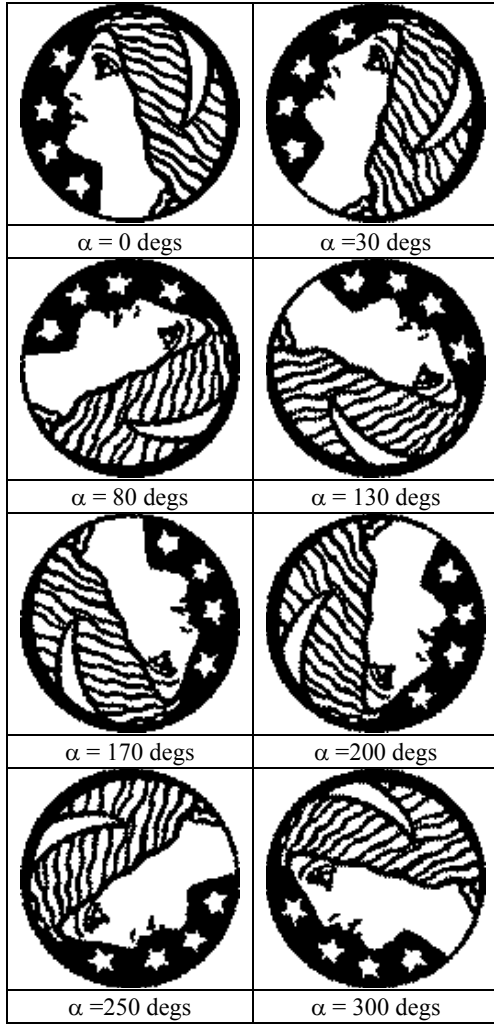


Fig. 3. A set of binary images used to analyse the invariant characteristics of radial Tchebichef moments.

The following tables give the values of the invariants  $\eta_p$ ,  $\eta_{pq}$  computed according to equations (19), (20). As seen from the data for different moments, invariants of type  $\eta_{pq}$  give better results compared to the type  $\eta_p$ .

| $\alpha$ | $\eta_{11}$     | $\eta_{53}$     | $\eta_{41}$     | $\eta_{22}$     |
|----------|-----------------|-----------------|-----------------|-----------------|
| 0        | 0.155005        | 0.023713        | 0.012869        | 0.042373        |
| 30       | 0.157814        | 0.024614        | 0.009467        | 0.043044        |
| 80       | 0.152861        | 0.020619        | 0.012801        | 0.042216        |
| 130      | 0.158502        | 0.024144        | 0.009246        | 0.042408        |
| 170      | 0.153557        | 0.022119        | 0.012885        | 0.040085        |
| 200      | 0.159577        | 0.022987        | 0.014243        | 0.040121        |
| 250      | 0.155937        | 0.023226        | 0.013687        | 0.042821        |
| 300      | 0.153642        | 0.021619        | 0.015513        | 0.03907         |
| Mean     | <b>0.155862</b> | <b>0.02288</b>  | <b>0.012589</b> | <b>0.041517</b> |
| St.Dv    | <b>0.002523</b> | <b>0.001348</b> | <b>0.002192</b> | <b>0.001513</b> |

Table.1. Radial Tchebichef invariants of the type  $\eta_{pq}$  computed using the binary images in Fig.3.

| $\alpha$ | $\eta_2$        | $\eta_3$        | $\eta_5$        | $\eta_8$        |
|----------|-----------------|-----------------|-----------------|-----------------|
| 0        | 0.107365        | 0.081262        | 0.112885        | -0.15066        |
| 30       | 0.108222        | 0.074894        | 0.111501        | -0.15994        |
| 80       | 0.10112         | 0.079969        | 0.103111        | -0.15015        |
| 130      | 0.111218        | 0.076341        | 0.107199        | -0.1609         |
| 170      | 0.103998        | 0.078689        | 0.105982        | -0.16018        |
| 200      | 0.108935        | 0.069292        | 0.102972        | -0.16976        |
| 250      | 0.098092        | 0.070015        | 0.10949         | -0.15575        |
| 300      | 0.09845         | 0.084444        | 0.112704        | -0.14286        |
| Mean     | <b>0.104675</b> | <b>0.076863</b> | <b>0.108231</b> | <b>-0.15627</b> |
| St.Dv    | <b>0.005014</b> | <b>0.005321</b> | <b>0.004034</b> | <b>0.00829</b>  |

Table.2. Radial Tchebichef invariants of the type  $\eta_p$  computed using the binary images in Fig.3.

The robustness of the invariants with respect to image noise has been studied by adding 5% salt-and-pepper noise to the image, two of which are shown in Fig. 4. The corresponding results for the values of  $\eta_{pq}$  are in Table 3. Comparing the values with those given in Table 1, we find that the standard deviations have not been severely affected, but remain within acceptable levels (<1%).

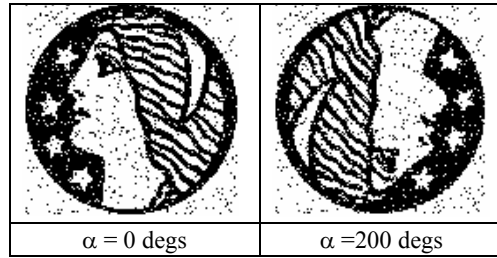


Fig. 4. Some of the input images with 5% salt-and-pepper noise.

| $\alpha$ | $\eta_{11}$     | $\eta_{53}$     | $\eta_{41}$     | $\eta_{22}$     |
|----------|-----------------|-----------------|-----------------|-----------------|
| 0        | 0.150981        | 0.0142          | 0.030386        | 0.030422        |
| 30       | 0.15245         | 0.026647        | 0.024253        | 0.04823         |
| 80       | 0.147177        | 0.022038        | 0.017943        | 0.049622        |
| 130      | 0.145947        | 0.021084        | 0.014364        | 0.029999        |
| 170      | 0.136533        | 0.032111        | 0.018129        | 0.031706        |
| 200      | 0.135932        | 0.02507         | 0.017941        | 0.037892        |
| 250      | 0.132575        | 0.013259        | 0.027235        | 0.051624        |
| 300      | 0.137397        | 0.034551        | 0.041193        | 0.035855        |
| Mean     | <b>0.142374</b> | <b>0.02362</b>  | <b>0.023931</b> | <b>0.039419</b> |
| St.Dv    | <b>0.007633</b> | <b>0.007633</b> | <b>0.008845</b> | <b>0.009063</b> |

Table.3. Radial Tchebichef invariants of the type  $\eta_{pq}$  computed for images with 5% noise.

The orthogonality property of a moment function can be verified by reconstructing the image from a given set of moments. In the case of a radial moment, the reconstructed image will have valid pixel values only inside the domain of definition of the kernel. Fig.5 shows the process of reconstruction for different values of 'pmax', using the first image in Fig.3.

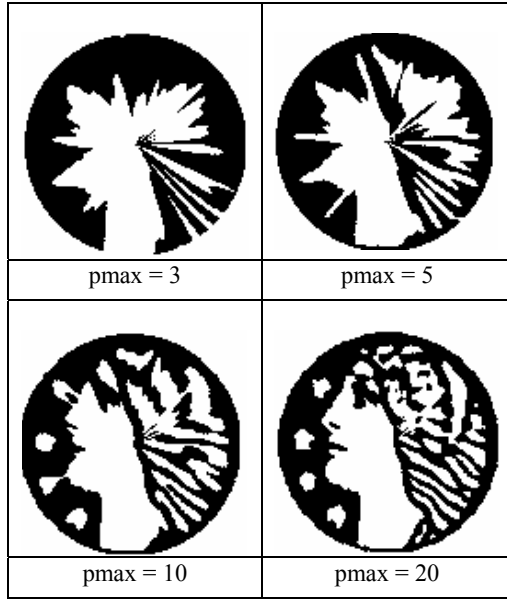


Fig.5. A set of reconstructed images using moments of orders up to 'pmax'.

A plot of the reconstruction error with respect to 'pmax' is shown in Fig. 6. The error was computed as the sum of absolute differences between the intensity values of the reconstructed image and the original image.

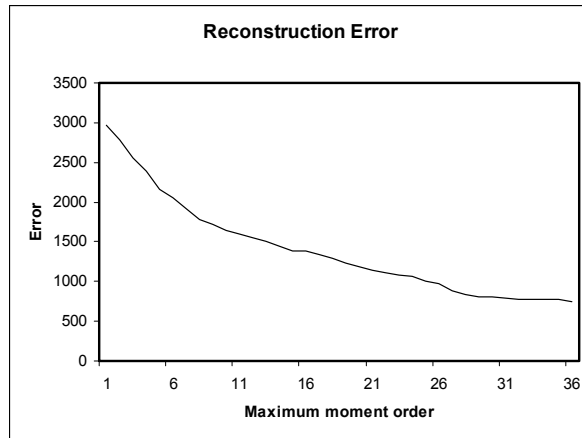


Fig. 6. Plot of reconstruction error (for a binary image) as a function of the masimum order of moments.

Grey-level images were also used to analyze the feature representation capability of radial Tchebichef moments. One of the images of size 128x128 pixels, used in the analysis and its reconstructions are shown in Fig. 7. The plot of the reconstruction error with respect to the maximum order of moments used, is shown in Fig. 8. The reconstruction error was computed as the root of sum of squared differences between the original and reconstructed intensity values.

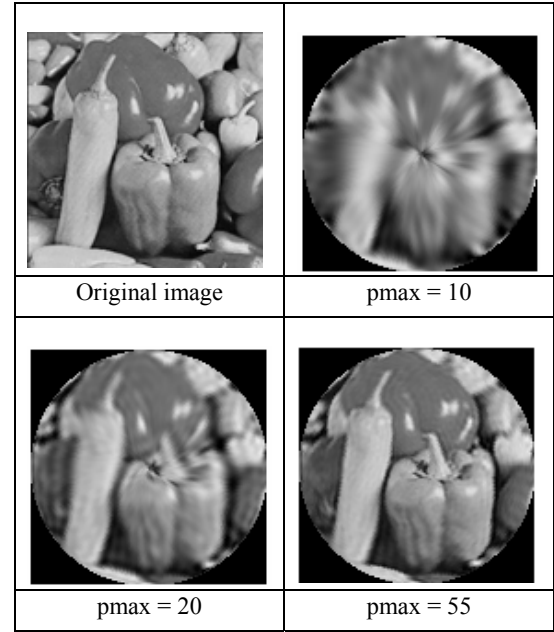


Fig.7. A gray-level image and a set of reconstructed images using moments.

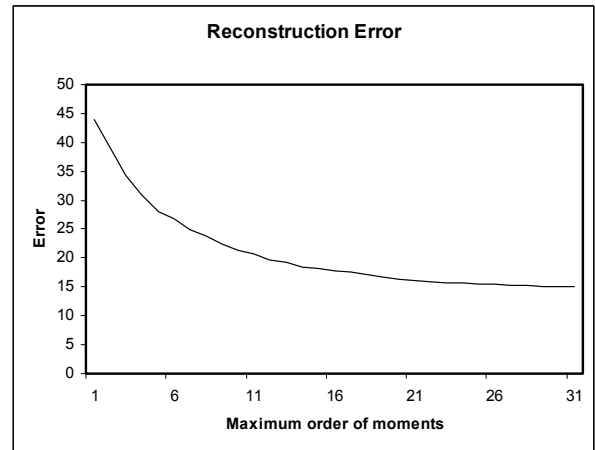


Fig. 8. Plot of reconstruction error (for grey-level image) as a function of the masimum order of moments.

## VII. CONCLUSIONS

The paper has presented the mathematical framework of a new set of moment functions called the radial Tchebichef moments. Discrete orthogonal moments based on Tchebichef polynomials were recently introduced for image analysis applications. The proposed framework of radial Tchebichef moments is based on the structure of Zernike moments, and is particularly suitable for pattern recognition tasks requiring rotational invariants. The important implementation related aspects and results showing the invariant and orthogonality characteristics of the moment functions have also been presented.

## REFERENCES

- [1] A. Khotanzad, "Invariant image recognition by Zernike moments," *IEEE Trans. Pattern Analysis and Machine Intelligence*, vol. 12, no. 5, pp. 489-497, 1990.
- [2] S.O. Belkasim, "Pattern recognition with moment invariants -A comparative study and new results," *Pattern Recognition*, vol. 24, no. 12, pp. 1117-1138, 1991.
- [3] M. R. Teague, "Image analysis via the general theory of moments", *J. Optical Soc. Of America*, vol. 70, pp. 920-930, 1980.
- [4] S. X. Liao, M. Pawlak, "On image analysis by moments," *IEEE Trans. Pattern Analysis & Machine Intell.*, vol. 18, pp. 254-266, 1996.
- [5] R. Mukundan, S.H. Ong, P.A. Lee, "Image analysis by Tchebichef moments," *IEEE Trans. on Image Processing*, vol. 10, no. 9, pp. 1357-1364, 2001.
- [6] A.V. Nikiforov, Suslov S.K, Uvarov V.B, *Classical Orthogonal Polynomials of a Discrete Variable*, New York: Springer-Verlag, 1991.
- [7] W. Gautschi, *Orthogonal Polynomials: Computation and Approximation*, Oxford University Press, Oxford, 2004.
- [8] A. Erdelyi *et al.*, *Higher Transcendental Functions*. New York: McGraw Hill, 1953, vol 2.
- [9] R. Mukundan, "Some computational aspects of discrete orthonormal moments," *IEEE Trans. on Image Processing*, vol. 13, no. 8, pp. 1055-1059, 2004.

**R. Mukundan** (SM'96) received the Ph.D degree from the Indian Institute of Science, Bangalore, India in 1996, for his research work on "Image based attitude and position estimation using moment functions". He was a senior scientist with the Control Systems Group at the Indian Space Research Organization (ISRO Satellite Centre, Bangalore, India) from 1982 to 1997. Later he joined the Faculty of Information Science and Technology at Multimedia University (MMU) in Melaka, Malaysia, where he held the positions of Associate Professor and the Chairman of the Centre for Mathematical Modeling and Computational Science, until December 2001. Currently, he is a senior lecturer in the Department of Computer Science at University of Canterbury, New Zealand.

The primary research interests of Mukundan are in the areas of moment based feature descriptors and their applications in computer vision, computer graphics algorithms, and image based rendering. He has authored a research monograph titled "Moment Functions in Image Analysis – Theory and Applications" published by World Scientific (Singapore) in 1998. He has also authored a book titled "Computer Graphics Algorithms in Java" which was published by Prentice-Hall (Malaysia) in 2000.